Journal of Marine Research, 61, 27–57, 2003

Seasonal to interannual upper-ocean variability in the Drake Passage

by Janet Sprintall[1]

ABSTRACT

Year-round monitoring of the upper-ocean temperature variability in Drake Passage has been undertaken since September 1996 through repeat expendable bathythermograph (XBT) surveys. The closely spaced measurements (6–15 km apart) provide the first multi-year time series for examining seasonal to interannual variability in this Southern Ocean choke point. While the temperature sections reveal the seasonal variability in water mass formation of the upper layer, there was no seasonal signal evident below 200 m. Similarly, there was little seasonal cycle evident in the position of the Subantarctic Front, the Polar Front and the Southern Antarctic Circumpolar Current Front associated with the Antarctic Circumpolar Current (ACC) in Drake Passage. Mesoscale eddy features are readily identifiable in the XBT sections and in some sparse salinity sections, as distinct alternating bands separated by near-vertical isotherms of cold and warm core temperatures. The eddies can also be tracked in concurrent maps of altimetric sea surface height, with time scales of ~35 days and diameters of 50–100 km, following a north to north-east trajectory with the main path of ACC flow through Drake Passage. Both the XBT and the altimetric data suggest the eddies are mainly confined to the Antarctic Polar Frontal Zone. To determine transport, an empirical relationship is derived between upper ocean XBT temperature and a baroclinic mass transport function from historical CTD casts collected in the Drake Passage. While in the temporal mean the strongest eastward transport is associated with the three major fronts in the ACC, the individual cruises strongly suggest a banded nature to the flow through the passage. Some, although not all, of the eastward and westward bands of transport can be attributed to the presence of eddies. The high spatial resolution of the XBT measurements is more capable of distinguishing these counterflows than the typical 50 km resolution of historical hydrographic sections across Drake Passage. Commensurate with the position of the fronts, no real seasonal signal in Drake Passage transport is discernible, although there is substantial variability on interannual time scales. The Drake Passage XBT transport time series is strongly correlated to both zonal wind stress and wind stress curl in the southeast Pacific Ocean.

1. Introduction

Within the Southern Ocean, the Antarctic Circumpolar Current (ACC) links the circulation of the Indian, Pacific and Atlantic Oceans, thus providing a global pathway for transferring interocean heat and freshwater anomalies. The ACC is characterized by

1. Scripps Institution of Oceanography, University of California, La Jolla, California, 92093, U.S.A. ***e-mail: jsprintall@ucsd.edu***

continuous circumpolar fronts, distinguishable by temperature gradients, that separate the distinctly subantarctic waters to the north from colder Antarctic water masses to the south (Orsi *et al.,* 1995). These fronts must squeeze together in Drake Passage, which at 700 km is the narrowest constriction through which the ACC must pass on its global journey. The Drake Passage has therefore provided a convenient choke point where the variability in mass and property fluxes of the ACC can be readily measured and studied.

The International Southern Ocean Study (ISOS) intensive field program from 1974–81 contributed much to our present knowledge of oceanography within the Drake Passage: the distinct zonation of the flow and water masses in the passage (Nowlin *et al.,* 1977); the coherence of the horizontal and vertical scales of velocity and temperature within the frontal regions (Pillsbury *et al.,* 1979; Sciremammano *et al.,* 1980); and the occasional horizontal excursions of the fronts through the formation of mesoscale meanders and current rings (Joyce *et al.,* 1978; Peterson *et al.,* 1982). In particular, the observance of the mesoscale features within Drake Passage during ISOS revolutionized our perception of the exchange of heat, salt and energy fluxes across the ACC, and further, plays a vital role in the dynamics of the ACC. Bryden (1979) suggested that the poleward oceanic eddy-heat flux was sufficient to balance the 0.4 pW heat lost to the atmosphere south of the Polar Front, as suggested by Gordon and Taylor (1975). This is supported by recent direct velocity measurements from a mooring array in the ACC south of Australia (Phillips and Rintoul, 2000). The eddies may also provide an effective mechanism for dissipating the energy input of the wind, furnishing a downward energy flux that balances the wind-driven eastward momentum in the ACC through topographic pressure drag (Bryden, 1979), although Morrow *et al.* (1994) suggest that the lateral divergence of eddy momentum flux may be too small and in the wrong direction to directly affect the momentum balance of the ACC.

A net transport for the ACC of 134 Sv was arrived at through a progression of studies of the hydrographic surveys, picket-fence of moorings, and the bottom pressure gauge data collected in Drake Passage during the ISOS experiment (Whitworth *et al.,* 1982; Whitworth, 1983; Whitworth and Peterson, 1985). This transport value has been used extensively by oceanographers, particularly in their quest for known constraints when employing large-scale inverse models (for example, Rintoul, 1991; McDonald, 1998 etc.). More recently, five conductivity-temperature-depth (CTD) occupations between 1993–2000 of World Ocean Circulation Experiment (WOCE) section SR1, located east of Drake Passage between the Falkland Islands (Burwood Bank) and Elephant Island (see Fig. 1), find remarkable agreement with the ISOS estimate with a mean transport estimate of 135.9 Sv relative to the bottom (Cunningham *et al.,* 2003). Cunningham *et al.* (2003) again reanalyzed the ISOS data and found the range of uncertainty about the mean net transport estimate was 35 Sv, and so much larger than the 10 Sv suggested by Whitworth and Peterson (1985). The size of the fluctuations suggest that the average transport value should be treated with some caution, as real variations due to different time scales of regional and remote forcing can severely alias mean estimates if the survey period is not long enough. In

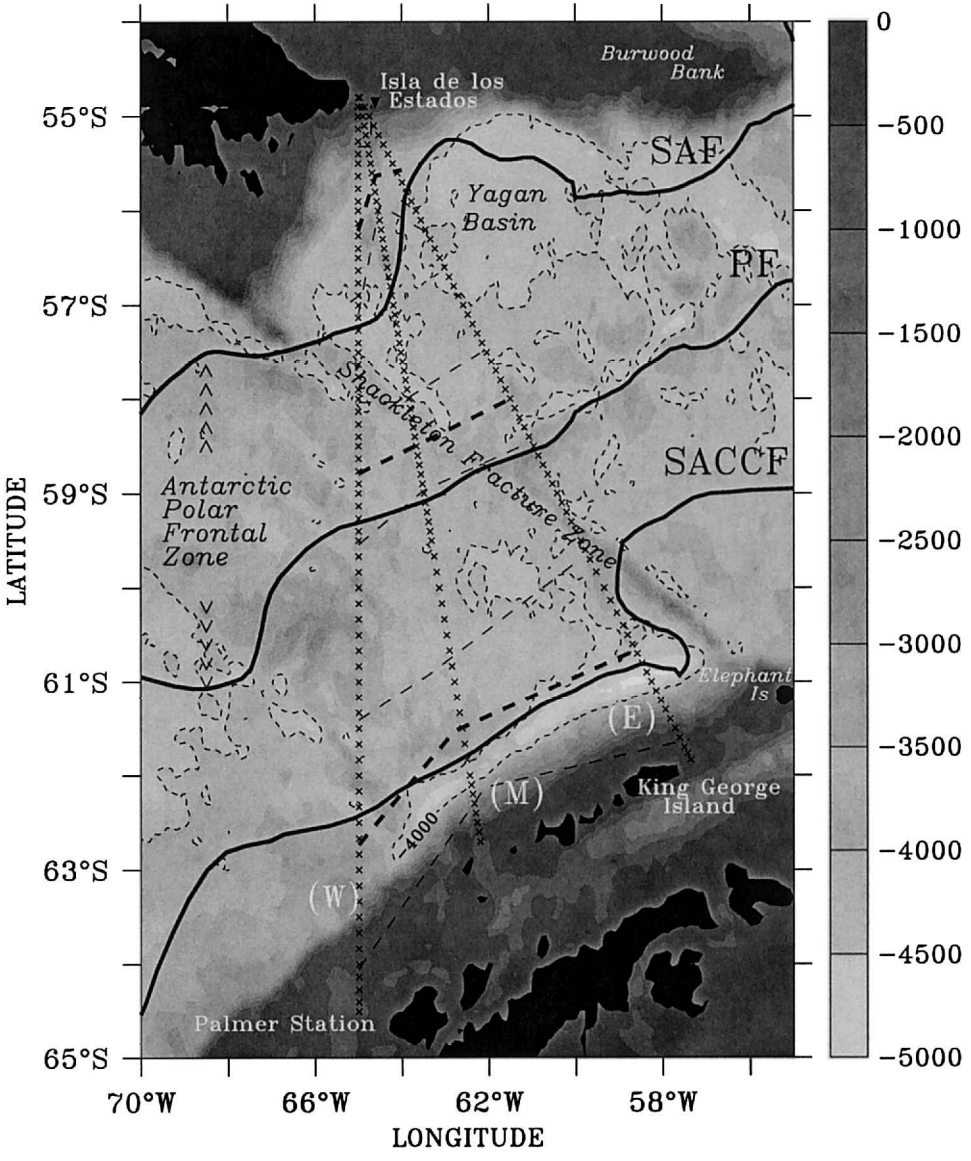

Figure 1. The average position of the high-density XBT drops (x) from the XBT program in Drake Passage mark the eastern (E), middle (M) and western (W) transects. The mean position (heavy dashed) and one standard deviation (light dashed) of the Subantarctic Front (SAF), Polar Front (PF) and Southern Antarctic Circumpolar Front (SACCF) from the XBT data, and from Orsi *et al.* (1995) (solid) are marked. The area between the SAF and the PF is the Antarctic Polar Frontal Zone. Bathymetry (m) from Smith and Sandwell (1997) is shaded, and the 4000 m contour is marked. Bathymetric and geographic features referred to in the text are labeled.

this paper, the variability of baroclinic transport estimated from the Drake Passage XBT sections is also shown to be large.

While the large-scale field effort during the ISOS program and the recent five discrete yearly WOCE surveys just east of Drake Passage supply vital information of the characteristics and structure of flow in the ACC, a continuous year-round monitoring effort is required to examine higher frequency time scales as well as the year-to-year variations in the mass and property fluxes. Such an effort was initiated in September 1996, with subsequent near bi-monthly, high-density sampling of upper ocean temperature via expendable bathythermograph (XBT) measurements taken routinely across Drake Passage. This paper describes the seasonal to interannual upper ocean variability in Drake Passage, from 1996 to 2001, from those high resolution XBT transects. The closely-spaced transects in time and space enable us to characterize the variability in the positions of the main fronts within the ACC in Drake Passage, as well as the development of any mesoscale features in the form of meanders and eddies that occasionally appear along the fronts. The sea surface height residual obtained from eight years of TOPEX/Poseidon altimeter measurements from 1992–2000, is used to further examine the frequency and propagation paths of eddies through Drake Passage. Information from the near 10-day repeat cycle of the altimetric data provides a strong complementary measurement to the subsurface XBT data set for examining the higher frequency variability in Drake Passage. Finally, an empirical relationship between upper ocean temperature and a mass transport function is derived to determine the baroclinic transport (relative to 2500 m) from the recent high density XBT sections, with only a relatively small error. Seasonal to interannual variability in the subsequent five year baroclinic transport time series for the ACC shows a substantial range through Drake Passage.

2. Data description

a. High-resolution XBT program

The Drake Passage high resolution XBT program has been in place since September 1996, and is part of a broader Pacific-wide network of high resolution XBT transects (for example, Sprintall *et al.,* 1995; Gilson *et al.,* 1998). The Drake Passage crossing generally takes about two–three days to complete, and typically about 70 XBTs are dropped per cruise. The nature of the vessel—to ferry support-personnel and supplies to the various bases on the Antarctic Peninsula, and the scientists who conduct their research in Antarctica—means that the track is not always exactly repeating. However, three main routes have emerged (Fig. 1), along which the 33 transects to date (December 2001) have been fortuitously partitioned fairly evenly. Sampling generally begins and ends at the 200 m bathymetry line, with probe separations of about 6–10 km across the Subantarctic and Polar Fronts, and 10–15 km elsewhere. The dense sampling ensures that all temperature changes occurring within the circumpolar flow are measured to capture most of the variance associated with the mesoscale features and frontal systems. Typically 6–7 XBT sections are sampled per year, separated in time anywhere from one week to three months.

The XBTs are Sippican Deep Blue probes and because of the slow ship speed, they generally return temperature data to their full depth rating of ~800 m. The depth is adequate to cover the upper ocean circulation within Drake Passage, although the ACC contains substantial geostrophic shear below 800 m that is not captured by this XBT's measurement. We will return to the missing deep baroclinic and the barotropic contribution to the flow in the Discussion section. The XBT data are corrected for the systematic fall rate error following Hanawa *et al.* (1995). After correction, the root-mean-square (RMS) depth error is approximately 1% of the depth due to random probe differences, while RMS error of the thermister calibration is around 0.05°C (Roemmich and Cornuelle, 1987). The individual XBT profiles are carefully quality-controlled to allow expression of the subtle temperature fluctuations within Drake Passage. Fine-scale structure of interleaving is evident in many of the temperature profiles, particularly in the frontal regions. In fact, the editing of the profiles was very much an iterative process until we amassed sufficient profiles during all seasons to become familiar enough with the rich structure in the temperature variability of Drake Passage.

Some early Drake Passage XBT transects also included sparse sampling with expendable conductivity-temperature-depth (XCTD) probes, that provide both temperature and salinity information to around 800 m. The XCTDs were carefully quality-controlled to eliminate spiking due to different response times in the measurements by the thermistor and conductivity sensors. Effects due to bubble adhesion on the XCTD conductivity cell results in a fresh salinity offset at the sea surface, typically decaying over the top 10 meters or so (Gilson *et al.,* 1998). This effect was corrected by assuming salinity reaches a constant value in the upper temperature mixed layer. The Drake Passage transects that have included XCTD salinity measurements have provided a wealth of insight into the vertical salinity structure and its relevance in defining the major frontal transport zones. In particular, when eddies were present in the Drake Passage, simultaneous XBT temperature and XCTD salinity data are found to be particularly important for defining the stratification of the upper layer in order to accurately determine the extent of water mass exchange.

b. TOPEX/Poseidon altimetric sea surface height

TOPEX/Poseidon altimetric data were used for the period from September 1992 through the end of 2000, from the first 346 orbital cycles of measurements. The altimetric measurements consist of the along-track sea surface height residual, calculated relative to the four year average between cycles 11 and 167 (1993–1996). The ground tracks are very closely spaced in Drake Passage as it is near the southern limit of the satellites orbit. Cross-over points of the ground track at 58S are zonally separated by 167 km. The along-track resolution is 6.2 km with a repeat cycle period of 9.916 days. The altimetric dataset is version v2000-01-18-AKH, and was provided by the Jet Propulsion Laboratory in Pasedena, California, with their usual corrections applied: standard instrumental errors, atmospheric tropospheric and isonospheric effects, and the inverse barometer effect (see Benada (1977) for further details). The University of Texas Tidal Model Version 3.0 was

applied for the ocean tidal correction, and the Oregon State University Mean Sea Surface State 1995 grid corrected drift in the satellite ground track (approximately ±1 km along each pass). The sea state bias, which is a function of significant wave height and wind speed and is therefore large in Drake Passage, was corrected based on the algorithm suggested by Gaspar *et al.* (1994). The RMS error in the altimetric sea level measurement is expected to be about 4.3 cm (Gilson *et al.,* 1998). Instrumental noise accounts for nearly half of this RMS error, with the rest equally due to atmospheric and sea state effects, and the orbit uncertainty.

Objectively mapped sea surface height residuals were constructed on a 1/6° latitude by 1/6° longitude grid by 10 days in time, in order to examine the temporal evolution of the sea level signature of the eddies that pass through Drake Passage. Following Bretherton *et al.* (1976), an exponential representation of the covariance function was assumed, having horizontal e-folding distance of 1° in space, an e-folding time scale of 20 days, and a signal-to-noise variance of 0.3. The mapping procedure introduces an RMS error of about 3 cm (Gilson *et al.,* 1998).

3. Temperature variability in Drake Passage

a. Definitions of the ACC fronts

The ACC in Drake Passage is characterized by a series of relatively narrow eastward flowing jets, separated by broader bands of flow (Nowlin *et al.,* 1977). Each jet is associated with a sharp temperature front, forming the boundary between different water masses. The closely-spaced sampling of the XBT probes across Drake Passage has been designed to resolve these fronts. In the following, the definitions for the three main fronts of the ACC in Drake Passage—which, from north to south are the Subantarctic Front (SAF), the Polar Front (PF) and the Southern ACC Front (SACCF)—are drawn from the large body of literature that ensued as a result of the ISOS experiment.

The SAF has been defined by Sievers and Emery (1978) as the maximum subsurface temperature gradient between 3°–5°C at 300 m depth. This definition also marks the southern extent of the Subantarctic Mode Water (McCartney, 1977). A popular definition of the PF is given by Botnikov (1963) as the northern extent of the 2°C isotherm at 200 m depth (Joyce *et al.,* 1978; Orsi *et al.,* 1995). It has been suggested that the PF can also be depicted as a surface front (Moore *et al.,* 1997), which is particularly attractive given the recent accession of satellite sea surface temperature (SST) data. However, the PF has a dynamic reason for its location, being the region where the cold Antarctic surface waters slide beneath the Subantarctic water masses to the north (Orsi *et al.,* 1995). Comparing a surface expression of the PF (defined by the strongest SST gradient across an XBT transect) with the subsurface expression (as defined by Botnikov, 1963), resulted in a wide disparity of location, particularly in summer months when there is strong heating of the near surface layer. There is closer agreement in winter when the 2°C isotherm outcrops directly into the surface layer. Thus, given the ready availability of subsurface temperature

data from the XBTs, in this paper we employ the PF definition given by Botnikov (1963), to allow the true dynamic expression of the PF. The zone to the north of the PF and the south of the SAF is referred to as the Antarctic Polar Frontal Zone (APFZ).

The SACCF represents the southern most eastward core of the ACC that carries waters with circumpolar characteristics, and is distinct from the subpolar regime farther south (Orsi *et al.,* 1995). The SACCF is defined by the southern most extent of the 1.8°C isotherm along the maximum temperature gradient between 200–500 m. In Drake Passage, it is also appropriate to distinguish the Continental Water Boundary (CWB) to the south of the SACCF, although in the past the CWB definition has often been somewhat entangled with that of the SACCF (Orsi *et al.,* 1995). As Orsi *et al.* (1995) note, the SACCF is a circumpolar frontal feature, whereas the CWB denotes a regional water mass boundary in Drake Passage. In the closely spaced XBT data the cold, subsurface slope water found south of the CWB is readily distinguishable from the relatively warmer circumpolar SACCF. We use the CWB definition of Sievers and Emery (1978), as the northern extent of temperature below 0°C, along the maximum temperature gradient between 150–500 m depth.

b. The XBT temperature sections

The objectively mapped temperature sections from each XBT cruise in Drake Passage are shown in Plate 1. The position of each front, as defined above and if present at the time of the survey, is marked on the top axis. In Plate 1 and the following, cruises are identified by four numbers consisting of the two-digit year and the two-digit month in which they occurred (for example, the July 2000 cruise is 0007). We have also denoted whether the transect was conducted on the eastern (E), middle (M) or western (W) designated track, according to Figure 1. (This is important in order to interpret the southernmost latitude of each temperature section, as the tracks extend farther south from west to east.) The five years of relatively dense sampling in space and time along the Drake Passage XBT transect enables the year-round evolution of the zonal fronts and their associated water masses to be examined in detail for the first time.

Beginning at the southern end of the transects, an isothermal layer of subzero water extending deep into the water column marks the northern limit of subpolar water in the CWB. The CWB is evident only in the eastern cruise track sections (for example, see cruises 9609, 9611, 9710, 9811, 9812, 9910, 0011 and 0110 in Plate 1). The CWB is not

Plate 1. Objectively mapped temperature sections from XBT transects across Drake Passage. The labels indicate the year and month of each survey, and whether the crossing was on the east (E), west (W) or middle (M) transect according to Figure 1. The location of the Subantarctic Front (red arrow), Polar Front (green arrow), Southern Antarctic Circumpolar Front (blue arrow) and the Continental Water Boundary (black arrow) if present at the time of the survey are marked. The temperature key is given, and the 0°C, 2°C and 5°C isotherms are contoured.

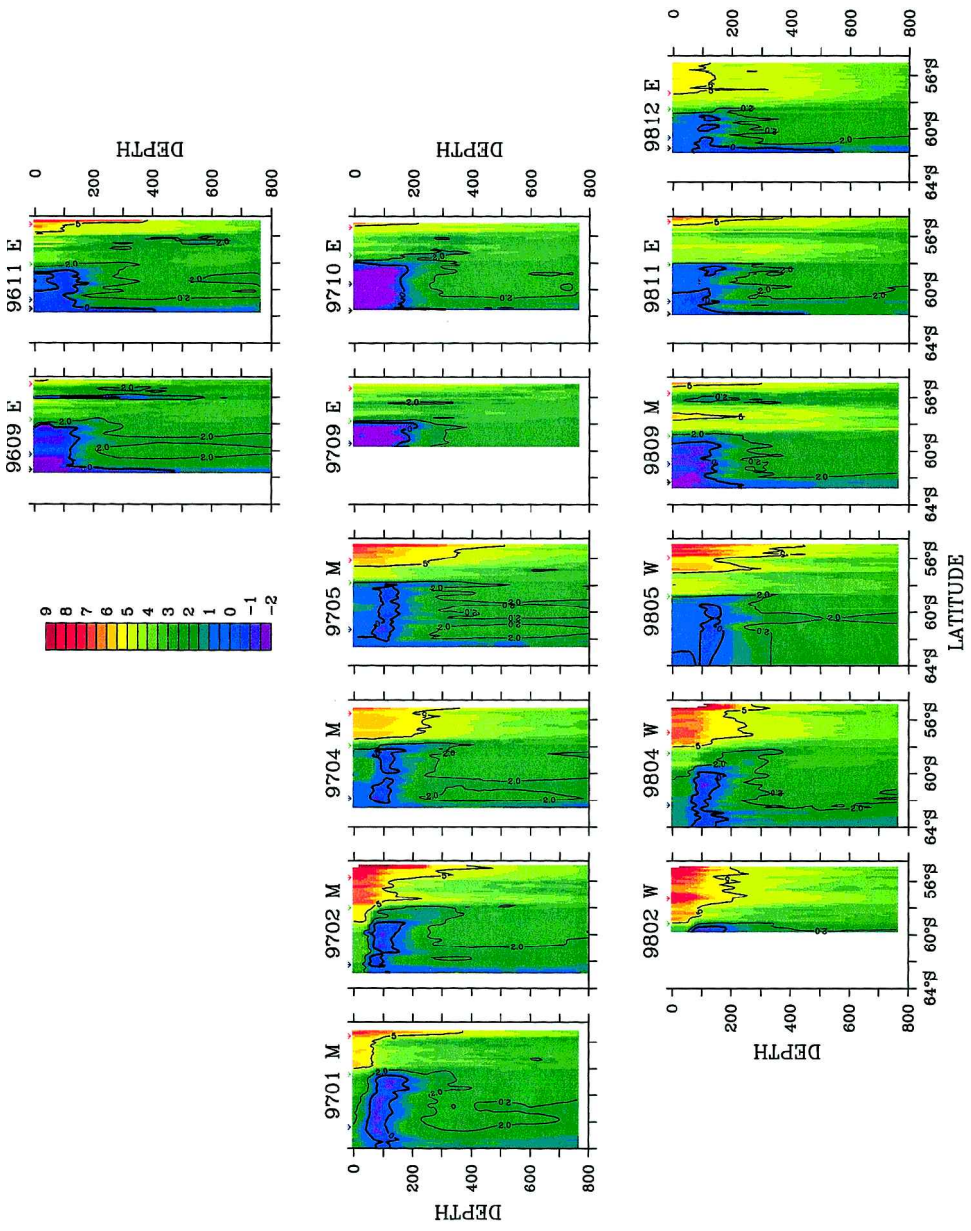
9701 M
9702 M
9704 M
9705 M
9709 E
9710 E
9802 W
9804 W
9805 W
9809 M
9811 E
9812 E
9609 E
9611 E
DEPTH
LATITUDE
64°S
60°S
56°S

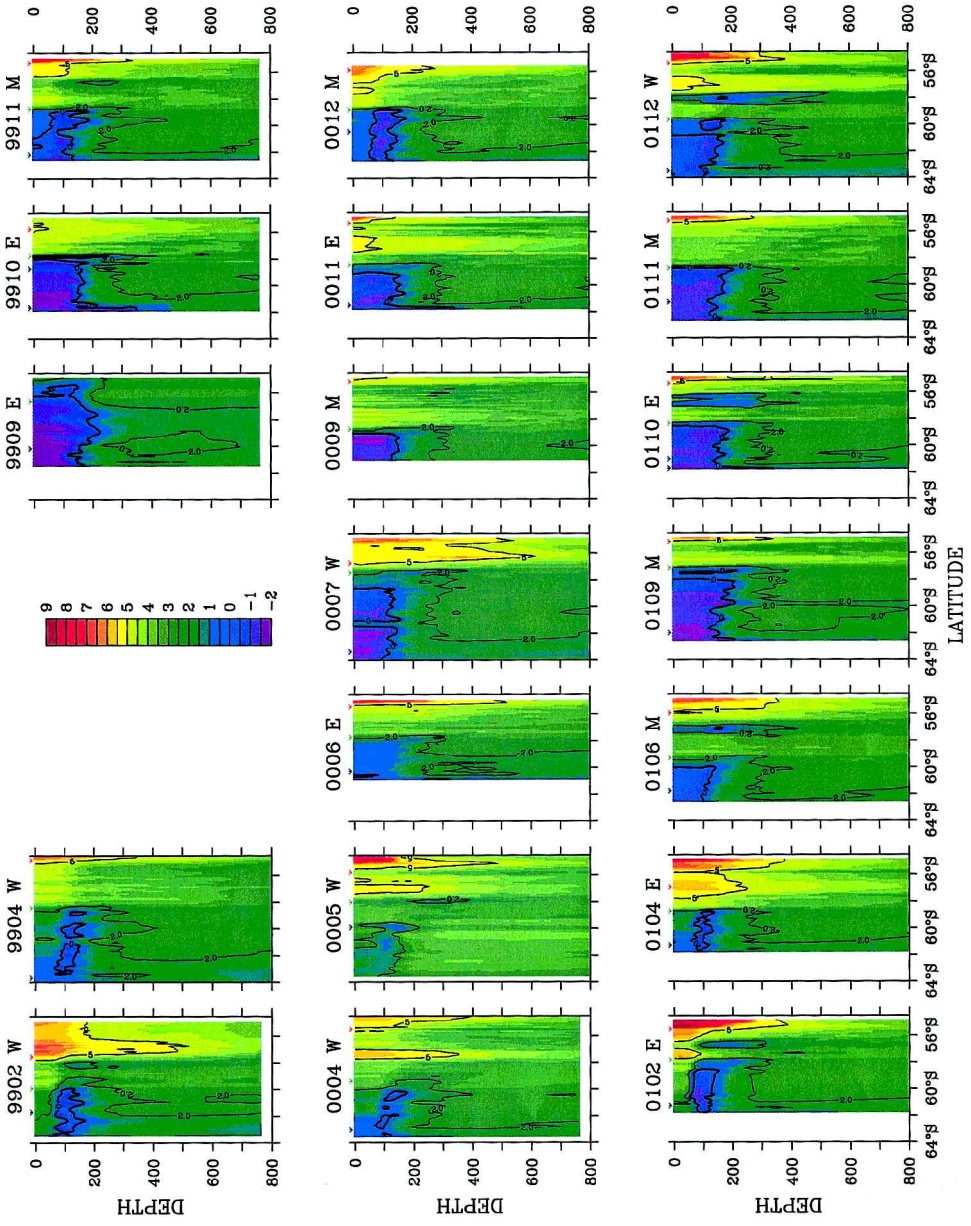
9902 W
9904 W
9905 W
9906 E
9907 W
9909 E
9910 E
9911 M
0002 W
0004 W
0005 W
0006 E
0007 W
0009 M
0011 E
0012 M
0102 E
0104 E
0106 M
0109 M
0110 E
0111 M
0112 W
DEPTH
LATITUDE
64°S
60°S
56°S
9
8
7
6
5
4
3
2
1
0
−1
−2

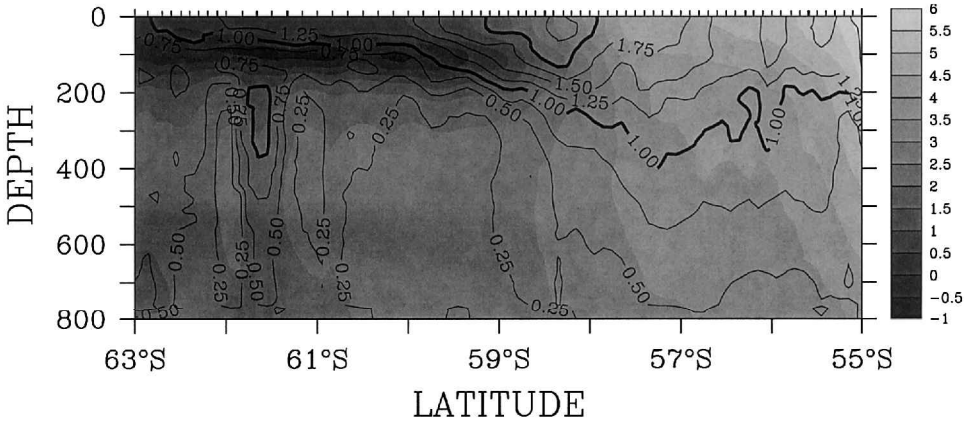

Figure 2. Average temperature (°C) with latitude from 33 transects of the Drake Passage XBT data, overlain with contours of the standard deviation. The mean position of the XBT probes are given on the top axis to show horizontal resolution of the temperature data.

found in any of the western or middle XBT cruise track sections. During the ISOS period, Sievers and Emery (1978) identified a CWB in eight Drake Passage XBT transects that closely correspond to our eastern cruise track, with no CWB evident in their three XBT sections that correspond to our western cruise track. The eastern distribution confirms the suggestion by Sievers and Nowlin (1988) that the cold continental slope water originates in northern Bransfield Strait. Further, the XBT transects in Plate 1 suggest that slope water is only present from the end of the austral winter until early spring, although with only five years of data we cannot discount real interannual variation. The local subsurface maximum in variability and the strip of colder water at ~61.7S in the mean temperature section of Figure 2 indicates the temporal presence of the slope water at this southern extent of the eastern cruise track.

North of the cold slope water lie the water masses and fronts that define the ACC. The SACCF is found on nearly all XBT transects (Plate 1). Historical CTD data in Drake Passage show the front may extend deeper into the water column below the 800 m depth reached by the XBTs (Orsi *et al.,* 1995). The SACCF partially consists of cold Antarctic Surface Water (AASW), formed at the surface during the winter months. The AASW is evident as the subzero surface layers extending to ~150 m depth in the late winter sections from September through November (Plate 1). Surface heating during the spring and summer traps the AASW to form the well-defined temperature minimum layer (temperatures < 0°C) centered at ~100 m depth from December through February (Plate 1). The seasonal change in the depth of the temperature minimum layer is depicted by high variability in the top 100 m of the mean temperature section (Fig. 2). In late summer-early fall (April and May sections in Plate 1), the temperature minimum layer consists of patches of warmer water that may have intruded from above, or through upwelling of warmer waters from below (Sievers and Emery, 1978). Below the AASW, the SACCF also

contains the Upper Circumpolar Deep Water (UCDW) mass. The UCDW is found on all sections, and is characterized by temperatures greater than 1.8°C (Orsi *et al.,* 1995). The UCDW occupies a substantial volume of the transect across Drake Passage, and shows the least temporal variability in temperature (<0.25°C) of all the water masses (Fig. 2).

The sharp temperature gradient evident in all sections, where temperature increases from the subzero AASW in the south by several degrees to the north, denotes the position of the PF (Plate 1). The position of the PF has the strongest temporal variability of all the ACC fronts with a standard deviation of >2°C between 58–59S and 0–100 m (Fig. 2). The closely spaced XBT profiles show the isotherms to be nearly vertical from the surface to ~300 m depth at the PF during late austral winter, but weakening in summer due to surface heating (Plate 1).

Within the APFZ between the PF and the SAF, the individual XBT profiles show much water mass interleaving and temperature inversions throughout the upper layer. Warm-core and cold-core eddy features frequently populate the APFZ (for example, see 9609, 9709, 9809, 0004, 0011, 0106, 0110 and 0112 in Plate 1). The spatial extent and depth of the eddy cores are well-resolved by the dense sampling of the XBT probes. These mesoscale features are ubiquitous within the Southern Ocean (Bryden, 1983), and will be discussed in more detail in the following.

North of the SAF, the warmer Subantarctic Surface Water (SASW) is found above the Subantarctic Mode Water (SAMW) which is characterized by a thermostad of 4°–5°C water in the 300–700 m depth range present in most temperature sections (Plate 1). The SAMW is formed by upper-level winter convection in the southeast Pacific Ocean (McCartney, 1977), and part of this Pacific inventory is probably transported eastward through Drake Passage. Similarly, the SASW is also formed locally in the southeast Pacific, just off the southern coast of Chile, and may be transported south and eastward across the South American continental shelf and through Drake Passage. Both SAMW and SASW are better indicated by salinity (Whitworth and Nowlin, 1987), and so a complete inventory in Drake Passage through the XBT program is not really possible. Local summer heating of the surface water may also contribute to the warm, upper mixed layers found north of the SAF during summer (see 9701, 9702, 9802 in Plate 1).

Figure 3 shows the average temperature for the 0–100 m, 200–400 m, and 500–700 m layers. Little difference is evident between the average temperatures over the two deeper layers. They range between 2°–3°C, temperatures that are probably indicative of the large area of UCDW across the section, and are slightly higher during the late austral summer. The upper layer (0–100 m) average temperature displays a distinct seasonal cycle: average temperature is higher in summer and lower in winter. During austral winter, the average temperature of the upper layer is lower than the layers below it, due to the formation of the AASW in the southern part of the section. The cool upper layer in September 1999 is due to the influence of the iceberg known as B10-A that calved off the Ross Sea ice shelf in 1997, and passed through Drake Passage during this cruise (see 9909 in Plate 1).

While the seasonal cycle is evident in the upper temperature structure across Drake

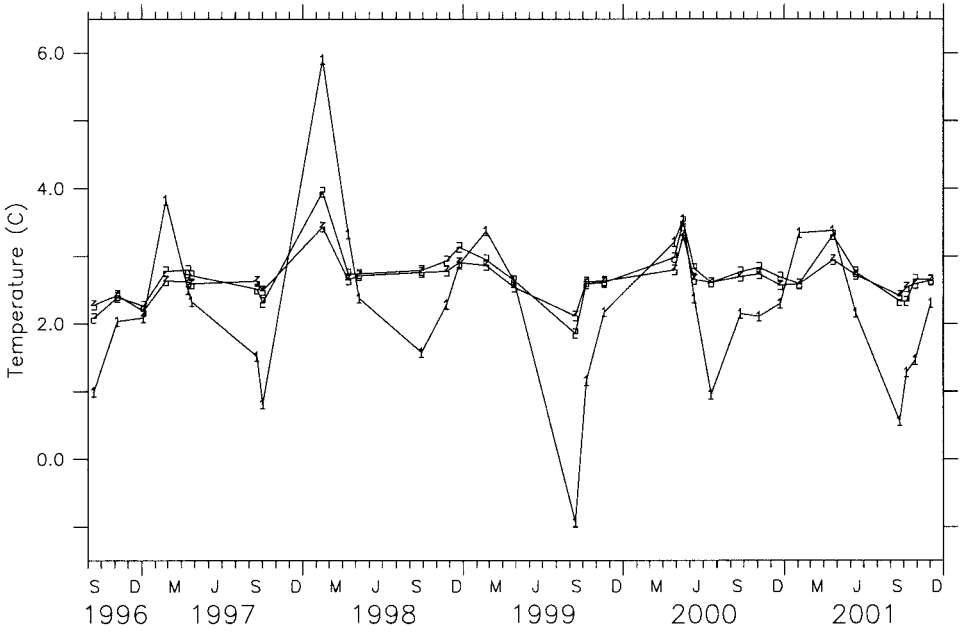

Figure 3. The average temperature across Drake Passage from each XBT transect for the 0–100 m layer (line-1), the 200–400 m layer (line-2) and the 500–700 m layer (line-3).

Passage, the position of the SAF or PF appears to be dominated by interannual changes (Fig. 4a). There is a slight tendency for the PF and SAF to act in concert, both being farthest south in austral summer, and farthest north in austral spring. However, because the position of the fronts vary according to which track was taken across Drake Passage (E, M or W in Fig. 1), it is difficult to partition temporal from spatial variability in their location. As we accumulate more transects along each track, the distinction between the temporal and spatial positions of the fronts will become better defined. We can however, discuss the separation between the fronts defined as the APFZ (Fig. 4b). Clearly there is little significant seasonal cycle in the width of the APFZ, although there is significant variation on interannual time scales. The mean difference between the fronts is 2.6° latitude, but the width may vary from 0.5° to 4° latitude (~50–400 km) over the period of only a few months. Contrary to historical opinion (Whitworth, 1980; Sievers and Emery, 1978; Hofmann and Whitworth, 1985), there appears to be no clear dependence in the width of the APFZ on the presence of eddies in a section (marked along the top axis of Fig. 4b).

The mean position of each front and its standard deviation along each of the three main XBT transects in Drake Passage are marked on Figure 1. The mean location of the SAF and the PF from the XBT surveys are farther north compared to their historical positions from Orsi *et al.* (1995), also marked on Figure 1, although they follow the same general southwest to northeast orientation through the passage and are close to being within one

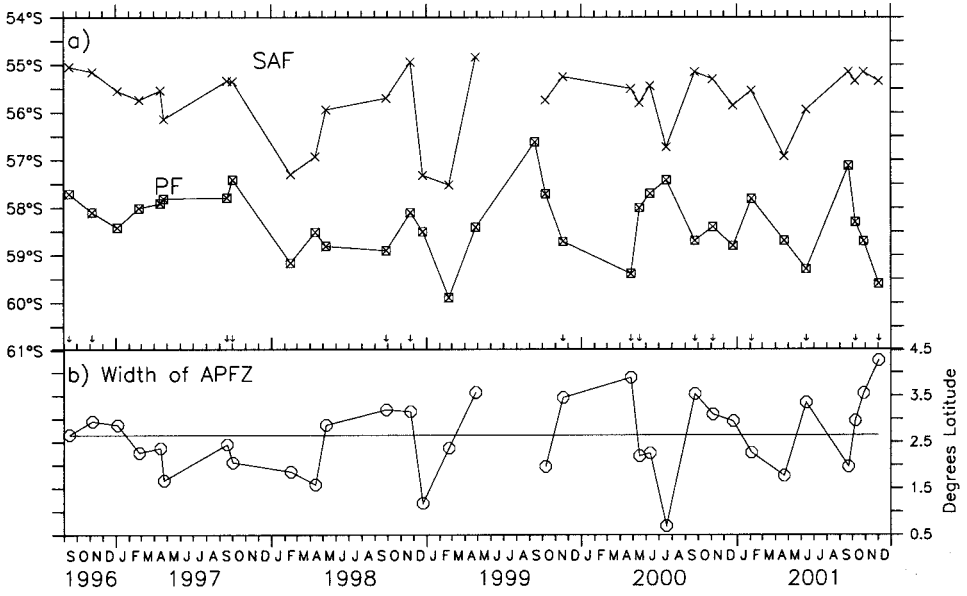

Figure 4. (a) The position of the Subantarctic Front (SAF) and the Polar Front (PF) from each XBT transect in Drake Passage. (b) The width of the Antarctic Polar Frontal Zone is the difference in degrees latitude between the SAF and the PF, and the average APFZ width of 2.6° is marked. The time of the XBT surveys that sampled eddy-type features are marked by arrows.

standard deviation. The mean position of the PF from the 5 year XBT data set is consistent with that found from the ISOS year-long mooring data in Drake Passage, where it ranged between 58.5S–59.5S (Hofmann and Whitworth, 1985).

4. Mesoscale variability observed in Drake Passage

Mesoscale variability in the form of meanders and eddies were observed within the APFZ and along the fronts in Drake Passage during the ISOS period (for example Joyce and Paterson, 1977; Legeckis, 1977; Nowlin *et al.,* 1977; Joyce *et al.,* 1981; Peterson *et al.,* 1982; Hofmann and Whitworth, 1985). Cold-core cyclonic eddies are thought to form from northward meanders of the PF, and thus contain water masses from the Antarctic zone (Nowlin *et al.,* 1977; Joyce *et al.,* 1981; Peterson *et al.,* 1982; Hofmann and Whitworth, 1985; Roether *et al.,* 1993), while warm-core anticyclonic eddies are thought to form from southward extensions of the SAF and therefore consist of water masses of a subantarctic origin (Gordon *et al.,* 1977; Hofmann and Whitworth, 1985). The high-density bi-monthly XBT program provides a rare insight into the seasonal to interannual variability associated with the mesoscale eddy features. In addition, the altimetric sea surface height data from the TOPEX/Poseidon satellite, which were not available to the earlier ISOS studies, contribute useful information for tracking the rings and examining their seasonality.

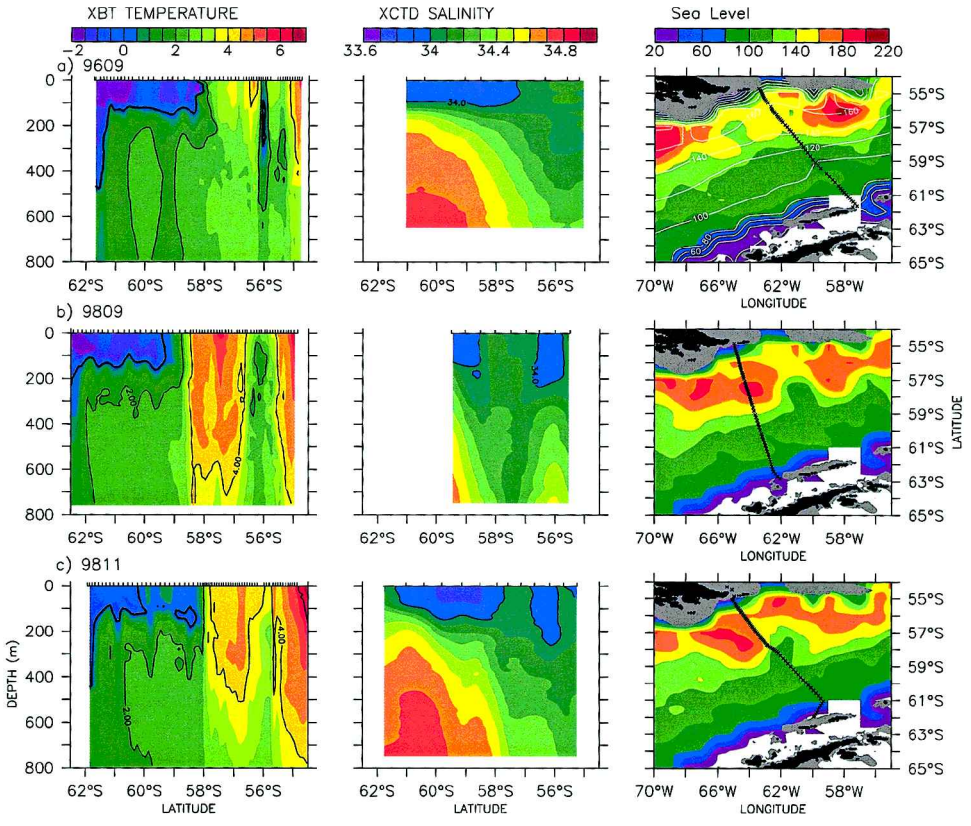

Figure 5. Objectively mapped contours of XBT temperature (left panels) and XCTD salinity (middle panels) from Drake Passage in (a) September 1996; (b) September 1998; and (c) November 1998. The XBT and XCTD probe locations from each survey are indicated along the top axis. Sea surface height elevation (right panels) is determined from the sum of the 0–2500 db dynamic height from the Olbers *et al.* (1992) atlas (white contours in right panel of 5a) plus the TOPEX/Poseidon sea surface height anomaly nearest in time to these Drake Passage cruises (marked by crosses).

When the eddies are present in the XBT temperature sections, their distinct bands of alternating warm and cool waters are readily distinguishable as the isotherms are nearly vertical and extend deep into the water column (for example, see 0004, 0106 in Plate 1). The spatial extent and depth of the cores are well resolved by the dense sampling of the XBT probes. The very first high-resolution XBT section across Drake Passage in September 1996, found very low to subzero temperatures sampled by 6 XBTs extending to ~500 m depth and centered around 56S, with warmer water found to the north and south within the APFZ (Fig. 5a). Sparse XCTD profiles from the same cruise suggest that the cold-core feature was relatively fresh (Fig. 5a). Similarly, XBT and XCTD sections in September 1998 (Fig. 5b) and November 1998 (Fig. 5c) also show cores of cold, fresh

water located at 56S, surrounded to the north and south by warmer and relatively saltier water. Although the XCTD sampling is too sparse to be conclusive, the September 1998 cold-core feature at 56S seems to be almost a mirror image of the thermohaline signatures found south of the PF from the surface to 800 m depth (Fig. 5b). These temperature and salinity sections strongly support the notion that the cold-core features consist of the same AASW water mass found south of the PF, whereas the warm water to the south of the cold-core feature has the same water mass characteristics as the SASW found north of the SAF. This confirms that rings may provide an efficient mechanism for water mass exchange meridionally across Drake Passage (Joyce *et al.,* 1978; Bryden, 1979).

It is difficult from the individual temperature sections to distinguish whether a cold-core feature is a cold-core eddy, or part of the recirculation from a warm-core eddy, or a meander within the ACC frontal system. However, the complete isolation of the thermohaline characteristics within the cold-core or warm-core features from their source waters to the north or south of the fronts, such as shown in Figure 5, strongly suggests that these features are indeed eddies. If the cold-core and warm-core features evident in the XBT temperature sections are eddies, then there should be an associated change in sea level elevation that is readily identifiable in the TOPEX/Poseidon sea surface height observations. In general, one expects a low sea surface height signature associated with a cyclonic cold-core eddy, and a high sea surface height associated with an anticyclonic warm-core feature. Indeed, the sea surface height observations from the pass nearest in time to each cruise in Figure 5, clearly show the depressions and elevations in sea level indicating the presence of the cold and warm-core features, respectively (Fig. 5, right panel). (Since the altimeter can only measure anomalous sea surface height, this map includes the 0–2500 db dynamic height determined from the Olbers *et al.* (1992) atlas (white contours in Fig. 5a) to give total sea level at the nearest time to the XBT survey.) These cases illustrate how the TOPEX/Poseidon sea surface height data, when combined with the XBT/XCTD data, may be able to capture the essential structure of the mesoscale features within Drake Passage.

The variance of the objective maps of TOPEX/Poseidon sea surface height anomaly shows an area of increased height in the northern part of Drake Passage that lies within the APFZ (Fig. 6). The highest region of sea surface height variability wholly occupies a relatively isolated (un-named?) deep basin, aligned with and to the east of the ridge that is the Shackleton Fracture Zone, and west of a deeper ridge that separates it from the Yagan Basin to the east-northeast (Fig. 1 and 6). The eastern most cruise track clips the western most part of the Yagan Basin, also within a region of relatively strong sea surface height variance. Also shown on Figure 6 are the maximum and minimum sea surface height anomalies from each of the 10-day TOPEX/Poseidon maps in Drake Passage. Clearly for the most part these extrema lie within the APFZ, especially given that the northern boundary (the SAF) determined from the XBT data actually lies further north than that found by Orsi *et al.* (1985) (see Fig. 1). Furthermore, Figure 6 also suggests that most of the extrema are found either directly within or east of Drake Passage. The region to the west of Drake Passage is relatively quiescent, at least with respect to mesoscale eddy variability.

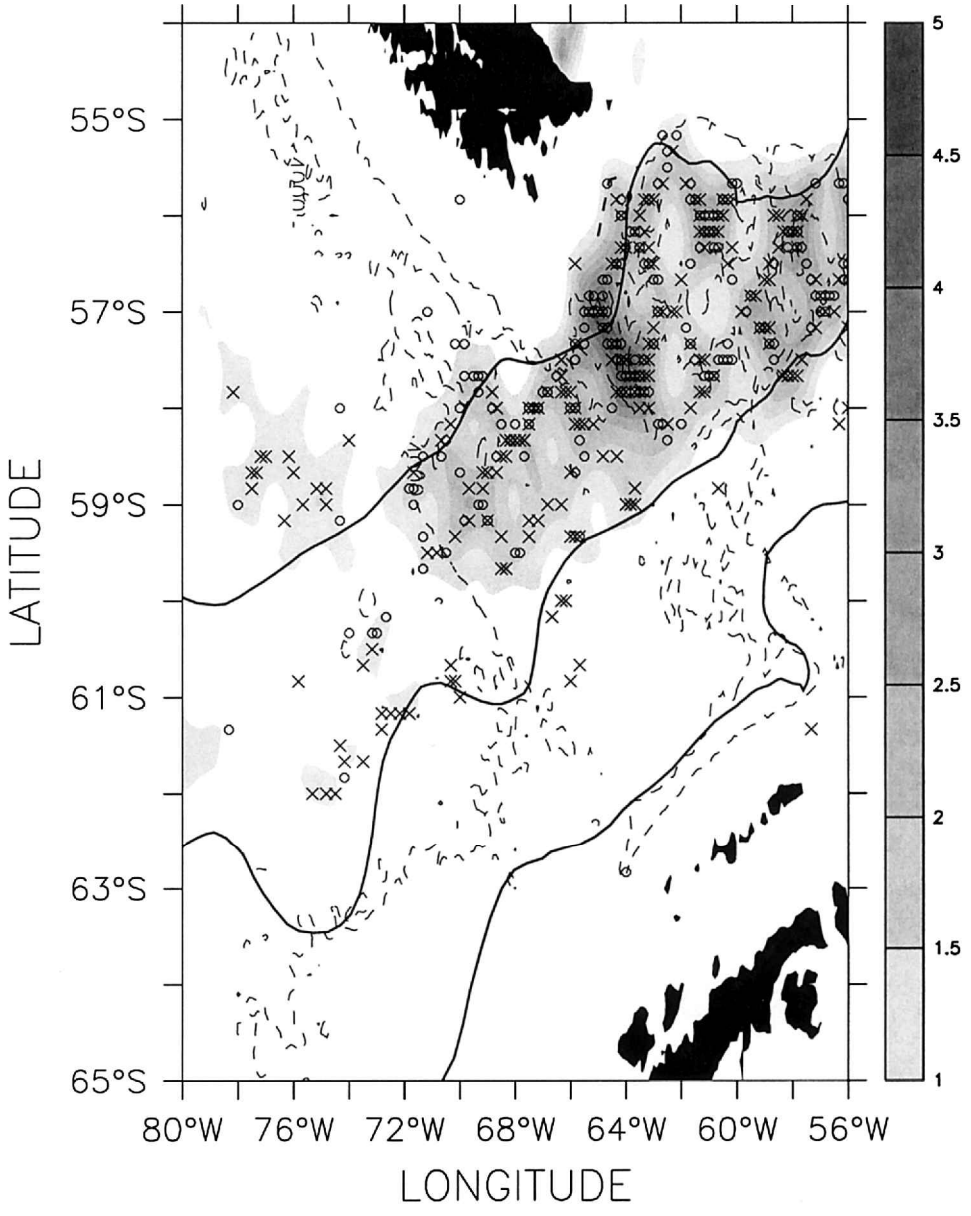

Figure 6. Variance of sea surface height (cm^2) estimated from 8 years of TOPEX/Poseidon sea surface height altimetric data in Drake Passage. The 4000 m bathymetric contour (dashed line) is from the Smith and Sandwell (1997) bathymetry. Heavy lines, from north to south, show the location of the Subantarctic Front, Polar Front and the Southern Antarctic Circumpolar Front from Orsi *et al.* (1995). Maximum (crosses) and minimum (circles) sea surface height extrema from each 10-day TOPEX/Poseidon cycle (with the seasonal cycle removed) are indicated.

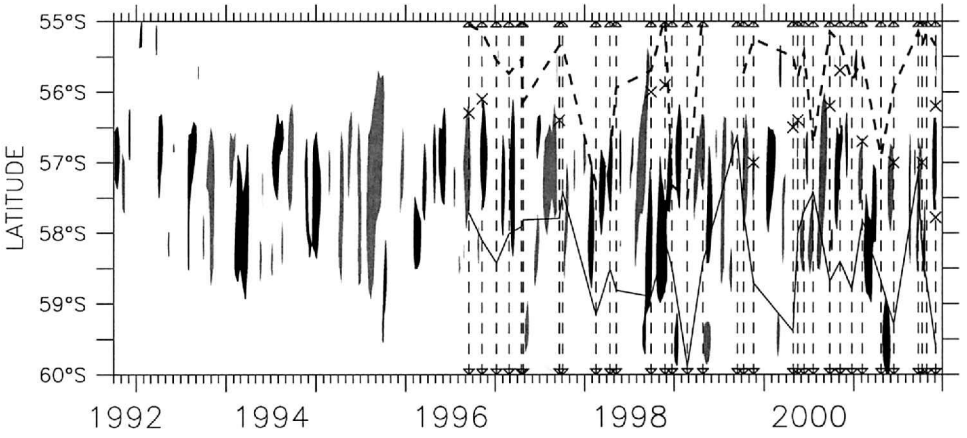

Figure 7. Time series of sea surface height anomalies along 65W in Drake Passage that are >20 cm (black) and < −20 cm (grey) from TOPEX/Poseidon altimeter data. The seasonal signal has been removed from the data. The central location of the cold-core features (crosses), the PF (solid line) and the SAF (heavy dashed line) as found at the time of each XBT temperature transects (dashed line) are marked.

The TOPEX/Poseidon sea surface height data have already proven very successful in many regions of the world oceans for the detection and tracking of eddies (for examples, see Goni and Johns, 2001; Feng and Wijffels, 2002). Sea surface height anomalies from TOPEX/Poseidon altimetric data in Drake Passage range from 60 cm to −60 cm. Joyce *et al.* (1981) determined a sea surface signature of ~20 cm associated with a cold-core eddy in Drake Passage during the ISOS period. Figure 5 also suggests sea surface elevations of ~20 cm associated with the eddies. Using a threshold anomaly of +(−)20 cm as indicative of warm (cold) core eddies, Figure 7 identifies the sea surface height anomalies lying outside these criteria along 65W between 55–60S. This longitude directly crosses the region of high variability in Figure 6, and corresponds to the western XBT cruise track. What is readily apparent from Figure 7 is, if the 20 cm threshold is a good indicator of the presence of eddies in Drake Passage, then they are indeed ubiquitous. Consistent with the XBT temperature transects in Plate 1, and the sea surface height variance of Figure 6, the identified eddies are primarily found within the APFZ between the PF and SAF, also marked on Figure 7.

The central location of the cold-core features from the XBT temperature sections are marked in Figure 7. Warm-core features are implicitly located to the north (but south of the SAF) and to the south (but north of the PF). The agreement in location of the eddy features from the two data sets is fairly good, especially for those cruises that lie on the western and middle transects and therefore are closest in alignment with this longitudinal slice of sea surface height data at 65W. At this longitude it appears that the individual eddies identified in the altimetric data set rarely last more than a month. The relatively short time scale of the eddies at 65W is also found in the time series of XBT temperature: the altimetric data

Table 1. Monthly census of warm core (sea surface height > 20 cm) and cold core eddies (sea surface height < −20 cm) from the 8-year TOPEX/Poseidon sea surface height data at 65W.

	56S		57S		58S	
	Warm	Cold	Warm	Cold	Warm	Cold
January	0	0	4	4	1	0
February	0	0	2	2	4	0
March	2	0	7	1	9	0
April	2	0	8	3	1	0
May	0	0	2	1	2	3
June	0	0	1	3	0	3
July	0	0	7	0	1	0
August	1	1	5	13	1	8
September	0	7	0	12	2	3
October	0	1	3	7	4	3
November	0	0	7	3	4	0
December	2	0	7	5	3	0

clearly suggests that the eddies are rarely present for more than two consecutive surveys which may be anywhere from 1–12 weeks apart (see Plate 1, and Fig. 3). A space-time spectral analysis of the Drake Passage sea surface height anomaly data indicates a time scale of ~35 days, and a length scale of ~50–100 km, which appears consistent with the XBT data. Figure 7 also suggests the slight northward propagation of the eddies at 65W, as indicated in Figure 6. This is consistent with the north-eastward alignment of the major frontal system (Fig. 1) and hence the ACC as it passes through Drake Passage.

A monthly census of warm and cold core eddies at 65W (Table 1) shows there is some seasonal variability in the presence of the eddies in the sea surface height time series of Figure 7. Cold-core eddies are most likely to occur during late winter to early spring, from August to October. Cold-core eddies in the APFZ are also observed during every single September XBT survey (Plate 1 and Fig. 5), except for September 1999 when the iceberg B10-A was present. Warm-core eddies at 65W showed more temporal variability, with a slight latitude dependence, and are generally present over the two month periods of March–April, June–July and November–December (Table 1).

5. Geostrophic transport from the XBT time series in Drake Passage

To calculate the geostrophic velocity and transport from the five-year time series of XBT temperature measurements it is necessary to first obtain an estimate of the steric height, relative to a specified reference level. Two techniques have emerged in the literature. The first assumes that temperature and salinity are well correlated, and so a mean T-S curve can be formulated using historical salinity data, and steric height is estimated from this salinity and the XBT temperature relative to their deepest common depth of typically ~800 m (for examples, see Gilson *et al.,* 1998; McCarthy *et al.,* 2000). This method is complicated in

the Southern Ocean, as inversions and frontal variability mean that the T-S relationship is not singular, and hence depth information with latitude must also be included. Furthermore, the subtle salinity variations within the eddies (Fig. 5) are not captured by the historical data. Uncertainty in salinity is the largest contribution to steric height errors on a large spatial scale, however this can be reduced through inclusion of simultaneous salinity measurement via XCTD sampling on individual cruises (Gilson *et al.,* 1998). At present, we have only five transects with XCTD salinity measurements. The XCTD sampling was reinstated at the end of 2001, and future studies will exploit the concurrent XBT and XCTD measurements for determining geostrophic flow in Drake Passage.

The second technique makes use of an appropriate relationship that links the subsurface temperature variability from the XBT data to some known (determined) structure function of steric height or mass transport. This technique has been used extensively for examining depth integrated flow in regions where there are only limited numbers of deep hydrographic stations but a copious number of shallow XBT subsurface temperature data (e.g. Ridgway and Godfrey, 1994; Rintoul *et al.,* 1997). In Drake Passage, we will use the historical CTD data to develop a mass transport function for the XBT time series that exploits a close correlation found between subsurface temperature and steric height from the CTD data.

The hydrographic data used in this analysis include CTDs in Drake Passage from the raw casts in the Southern Ocean Data Base (Olbers *et al.,* 1992). In all, 259 casts deeper that 2500 db were retained for a region that was 1 degree in longitude larger than the "triangle" formed by the three XBT transects that cross Drake Passage (Fig. 1). From each CTD cast we calculate the steric height at the usual standard depths relative to 2500 db, and determined the mass transport function to be the vertically integrated steric height from the surface to 2500 db (Q_{2500}),

$$Q_{2500} = g^{-1} \int_{p(2500)}^{p(z)} \delta(S, T, p) dp.$$

The 2500 db reference level is chosen as a compromise to incorporate an optimal number of CTD stations, and also appears to be an appropriate reference depth as determined by the historical analysis of baroclinic transport in the region (Whitworth and Peterson, 1985). In the past, most investigators have employed a simple linear best-fit regression relationship between the mass transport function and a single temperature variable, both from the same hydrographic station, to determine an empirical relationship for geostrophic transport from the XBT data. For example, Ridgway and Godfrey (1994) simply regressed the mass transport function against temperature at 450 m, and Rintoul *et al.* (1997) regressed dynamic height against the average temperature from the surface to 600 m. For this study in Drake Passage, we make use of the variation of temperature with depth, and employ a multivariate regression relationship between Q_{2500} and the temperature at 100 m (T_{100}), 400 m (T_{400}) and 700 m (T_{700}) depth for each CTD cast. The multivariate relationship

finds a high correlation (~0.9) between Q_{2500} and the T_{100}, T_{400} and T_{700} values. The RMS difference between the actual Q_{2500} of each cast and the Q_{2500} estimated from the regression fit is 7 m^2. Sensitivity studies using multivariate regressions for temperature at different depths, or averaged temperature over different depth ranges, did not substantially improve the correlation, nor the RMS error. Most likely the temperature at the depths chosen represent real vertical changes in the temperature structure: 100 m represents the upper layer and particularly the seasonal changes in the vertical extent of the upper layer AASW; 400 m represents the top of the UCDW layer; and 700 m is realistically the deepest common depth of all available XBT data and lies within the UCDW. We also experimented by dividing the Drake Passage CTD data into subregions. Scatter plots of Q_{2500} versus temperature showed a slight break in the tight fit at ~1.5°C, which suggests that two separate regimes either side of the PF may be more appropriate for determining the regression. Subdividing the data into two subregions based on the mean location of the PF decreased the rms error in both regions to ~6 m^2, however the correlation coefficient between Q_{2500} and temperature dropped to 0.82 for the southern subregion (161 CTD casts), and remained at 0.9 for the regression relationship determined from those CTDs north of the PF (96 CTD casts). Thus, for the sake of simplicity we determined that a single multivariate relationship,

$$Q_{2500} = 47.25 + 4.76T_{100} - 2.54T_{400} + 28.47T_{700} \quad (1)$$

is representative of the close correlation that exists between subsurface temperature and steric height within Drake Passage.

To validate the skill with which the multivariate relationship (1) can determine the mass transport function Q_{2500} from XBT temperature data alone, we use 3 hydrographic cruises from the ISOS period: the R/V *Melville* II cruise in February–March 1975; the R/V *Melville* V cruise in March 1975 and the R/V *Thompson* cruise in February–March 1976 (Nowlin and Clifford, 1982). Figure 8 shows the comparison of Q_{2500} calculated from each CTD cast with that estimated from (1), for each cruise. The agreement between the curves is remarkable. The RMS difference between the two estimates is 4.5 m^2, 6.3 m^2 and 7.1 m^2 for the *Thompson, Melville* II and the *Melville* V cruises, respectively. For comparison, the difference in the mass transport function across the Drake Passage sections is of the order 90 m^2. This suggests that the empirical relationship (1) can be used to determine the baroclinic transport (relative to 2500 db) from the five year Drake Passage time series with only a relatively small error.

The geostrophic surface component of the depth-integrated flow across the passage can be estimated directly from the horizontal gradient of Q_{2500} given in Eq. (1) (multiplied by g/f), and is shown for each XBT transect in Figure 9. The position of the major fronts in Drake Passage, if present at the time of the surveys, are also marked in Figure 9. The geostrophic surface transport for each cruise strongly suggests a banded nature to the flow through the passage. Alternating eastward and westward bands are evident across the sections, although in general the strongest eastward flow is found at the location of the SAF

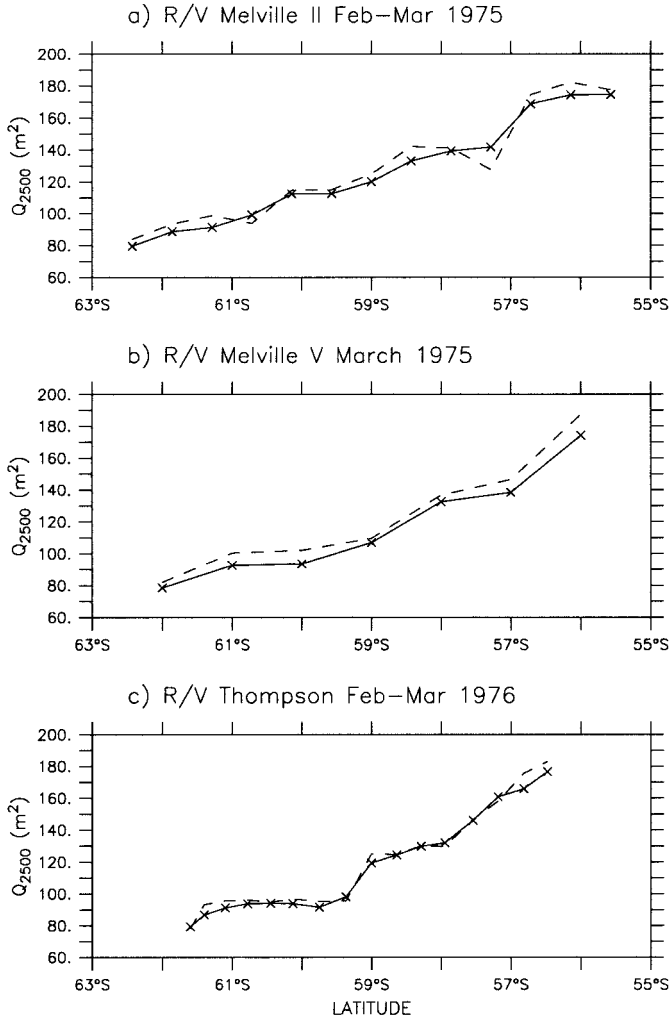

Figure 8. The mass transport function Q_{2500} (m^2) for the Drake Passage transects of the a) R/V *Melville* II cruise in February–March 1975; b) R/V *Melville* IV cruise in March 1975; c) R/V *Thompson* cruise in February–March 1976; estimated from the regression relationship given in equation [1] (dashed line), and the true value from the temperature and salinity data at each CTD position (crosses) during the cruise.

and the PF. In most cases, but not all, the strongest counterflows within the APFZ can be attributed to the presence of the eddies (e.g., 9609, 9809, 9911, 0004). Sections in Figure 9 also give a sense of the rotation about the eddy, such as in 0106 (0004) when there is an anticyclonic (cyclonic) eddy, centered around 56.8S (57.2S), that corresponds to the location of the cold-core (warm-core) features in Plate 1. However, since we have no

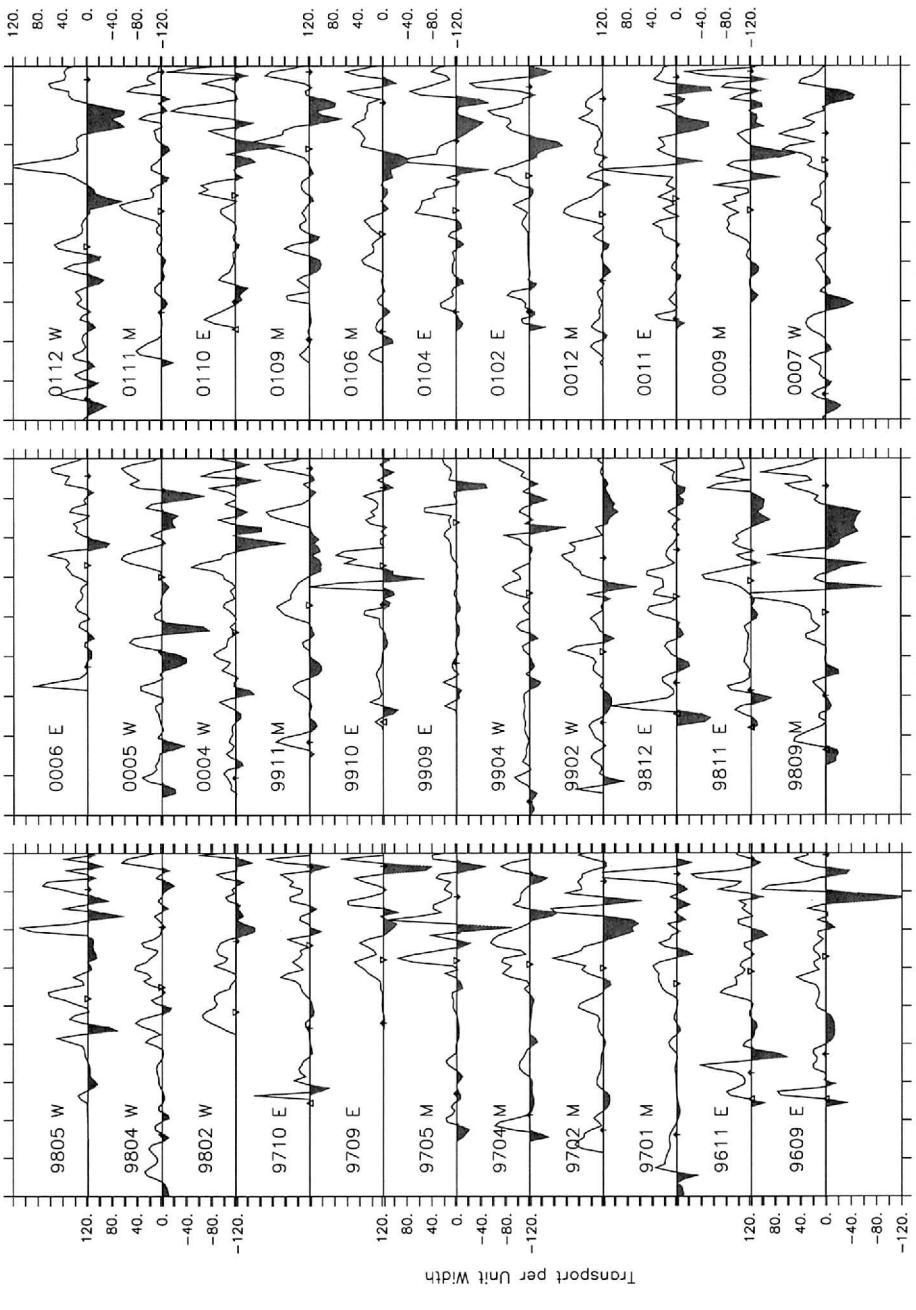
9805 W
9804 W
9802 W
9710 E
9709 E
9705 M
9704 M
9702 M
9701 M
9611 E
9609 E
0006 E
0005 W
0004 W
9911 M
9910 E
9909 E
9904 W
9902 W
9812 E
9811 E
9809 M
0112 W
0111 M
0110 E
0109 M
0106 M
0104 E
0102 E
0012 M
0011 E
0009 M
0007 W
120.
80.
40.
0.
-40.
-80.
-120.
64°S
62°S
60°S
58°S
56°S
LATITUDE
Transport per Unit Width

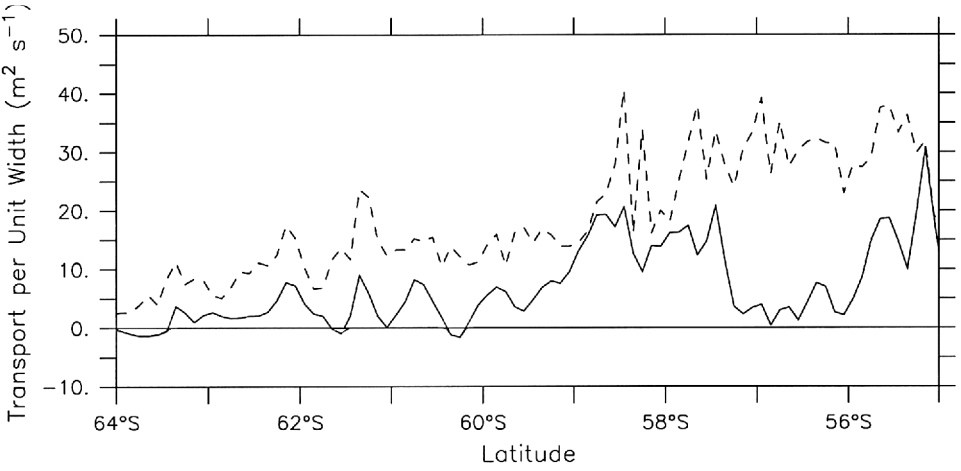

Figure 10. The temporal average geostrophic transport per unit width from the XBT sections (solid line) and its standard deviation (dashed line). Negative transport per unit width indicates westward flow, and is shaded grey.

concurrent horizontal water mass information it is difficult to ascertain if an eddy was completely surveyed by an XBT transect. In some cases we may only be clipping the edge of an eddy. In 0112, both the temperature section (Plate 1) and the geostrophic transport (Fig. 9) suggest that there may be two eddies: a cold-core cyclonic eddy lies poleward of a warm-core anticyclonic eddy.

In the temporal mean transport for the whole section the eastward flow associated with the three main fronts in Drake Passage is evident (Fig. 10), and separated by regions of weak or westward transport. The strongest eastward transport is associated with the SAF, although this region also has strong variability (Fig. 10). Relatively strong temporal variability in transport is also found within the APFZ, as expected with the frequent occurrence of eddies in this zone.

Poleward of the CWB, when it is present on the XBT sections, there is usually westward transport (for example, see 9809, 9812 in Fig. 9). The westward flow near the Antarctic continental boundary also appears in the mean transport for the section (Fig. 10). This counterflow was observed at two slope moorings deployed during ISOS for nearly the

←

Figure 9. The transport per unit width ($m^2 s^{-1}$) estimated from the gradient of the mass transport function given in Eq. (1) (multiplied by g/f), from the XBT temperature data. The labels indicate the year and month of each survey, and whether the crossing was on the east (E), west (W) or middle (M) transect according to Figure 1. The location of the Subantarctic Front (down arrow), Polar Front (down triangle), Southern Antarctic Circumpolar Front (up arrow) and the Continental Water Boundary (up triangle), if present at the time of the survey, are indicated. Positive transport per unit width indicates eastward flow and negative (shaded grey) indicates westward.

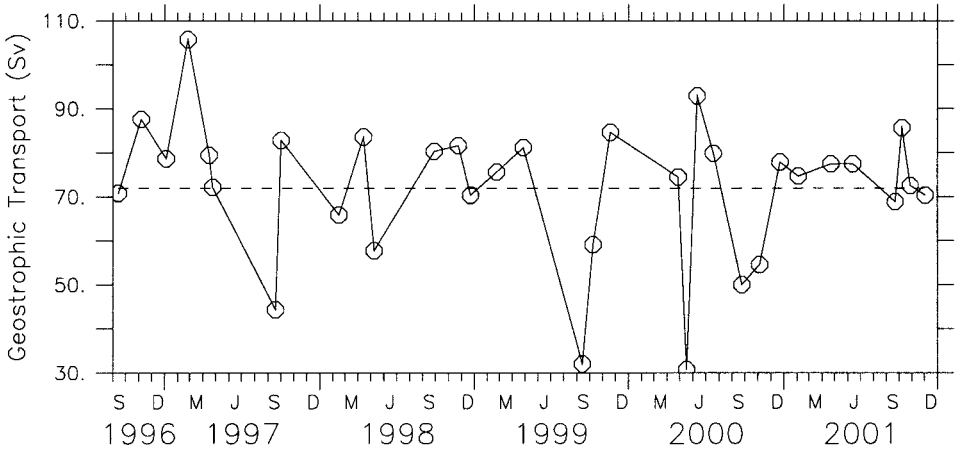

Figure 11. The time series of net geostrophic transport (10^6 $m^3 s^{-1}$) estimated from the integration of Eq. (1) (multiplied by g/f), obtained from the XBT temperature data.

entire year-long record (Nowlin and Zenk, 1988), and in the geostrophic transport estimated from three of the ISOS hydrographic sections (Whitworth *et al.,* 1982). These authors suggested this westward flow is the Antarctic Continental Slope Current, set up in response to the continental east wind drift near Antarctica.

The total net geostrophic transport through Drake Passage (Fig. 11) is obtained by integrating the mass transport sections in Figure 9 across each section. The five-year time series shows variability on interannual time scales, and commensurate with the position of the fronts (Fig. 4) no real seasonal signal is discernible. Similarly, there is no consistent effect on the net geostrophic transport of a section when an eddy is present. For example, in 9609 and 0112 when eddies were observed in the temperature sections (Plate 1), the total net geostrophic transport across the Drake Passage was near average. Whereas in 0009 and 0110 when there were eddies present in the APFZ (Plate 1), the net geostrophic transport is respectively weaker and stronger than average. Again, this may be a consequence of the way the eddies were surveyed.

The average geostrophic transport across Drake Passage is 71 Sv, with a range from 30 Sv to 105 Sv and a standard deviation of 15.3 Sv. The mean from the five-year XBT time series is in fairly good agreement with the 87 Sv average baroclinic transport (relative to and above 2500 db) determined from a one-year mooring deployment during ISOS (Whitworth, 1983), although the ISOS data ranged from 70–100 Sv. Short period fluctuations of ~15 Sv over two weeks were not unusual in the ISOS time series (Whitworth, 1983). Net geostrophic transport estimated from ISOS hydrographic sections (relative to and above 2500 db) were ~88 Sv (Nowlin and Clifford, 1982). Whitworth (1980) found little seasonal difference in net geostrophic transport: 79 ± 13 Sv from 16 summer hydrographic sections, and 71 ± 15 Sv from six winter sections (relative to and above

2500 db). Similarly, there is no obvious seasonal trend in the five-year geostrophic transport time series derived from the XBT data. The standard deviation of the XBT transport time series also agrees with 15.5 Sv from the ISOS data recently reported by Cunningham *et al.* (2003).

6. Discussion and conclusions

a. Temperature variability is mainly interannual

A unique time series of temperature measurements from a near bi-monthly XBT transect across Drake Passage reveal seasonal to interannual variability in the upper ocean characteristics of the Southern Ocean choke point. The five years of relatively dense sampling in time and space enables the evolution of the zonal fronts and their associated water masses to be examined in detail for the first time.

The temperature sections show distinct signatures of the seasonal cycle in the upper layer: formation of the temperature minimum AASW in the southern surface layer in winter; the patchiness of the AASW at ~150 m depth during spring; and the capping of the AASW in the south and the warming of the surface layer to the north in summer. However, there was no real seasonal signal evident below 200 m, and the time series of mean temperature in the 200–400 m and 500–700 m layers showed little trend or variation in the five-year time series. Similarly, there was little seasonal cycle evident in the location of the three major ACC fronts in Drake Passage, nor the width of the APFZ between the SAF and the PF. Rather, year-to-year variations dominated the time series.

The mean location of the SAF and PF within Drake Passage were farther north than their historical positions (Orsi *et al.,* 1995). Donohue *et al.* (2001) also found their SAF location in the Southern Pacific differed by as much as 3°–4° latitude from that determined by Orsi *et al.* (1995). This probably suggests that closely-spaced hydrographic data, as well as a sufficiently long enough climatological time series, such as provided by the Drake Passage XBT data, are required to determine the true location of the ACC fronts within Drake Passage.

b. Eddies frequently populate the Antarctic Polar Frontal Zone

Mesoscale variability, in the form of cold and warm-core eddies, are readily identifiable in the XBT temperature and some sparse XCTD salinity sections. The eddies are manifested in the sections by alternating bands of cold and warm core temperatures that are isolated and distinctly different from adjacent water masses, and in many cases extend to the 800 m depth resolved by the XBT probe. The eddies were only found within the APFZ, between the SAF and the PF, over the five-year XBT time series. Contrary to historical opinion, the eddies when identified in an XBT section, appear to have no consistent effect on the width of the APFZ. The eddies suggest an efficient mechanism for meridional water mass exchange across the APFZ within Drake Passage (Joyce *et al.,* 1978; Bryden, 1979), and this is supported in the thermohaline structure of the XBT and XCTD transects presented here (Fig. 5).

While previous field programs in Drake Passage have observed and analyzed these eddies in great detail, the addition of the altimetric sea surface height data from the TOPEX/Poseidon satellite launched in 1992 contributes valuable information for determining the spatial and temporal evolution of the rings that was not available to the earlier studies. Comparison between the location of the eddies from the XBT and XCTD data with the changes in sea level elevation that may also indicate an eddy location are promising. As found in the XBT data, the extrema of the sea surface height data were also primarily confined to the APFZ (Fig. 6). In the altimetric data, both high and low sea surface height features appear to weaken and move north to northeastward in time within the APFZ, suggesting speeds of around 20–30 cm/s. The anomalous sea surface height variability is highest in an un-named basin just east of the Shackleton Fracture Zone, and also in the Yagan Basin. During ISOS, seamounts and ridges in northern Drake Passage were thought to influence the amplitude and speed of the rings (Hofmann and Whitworth, 1985). The altimeter data clearly indicates that the appearance, trajectories and residence time of the eddies within Drake Passage are significantly influenced by these topographic features. Although, as an aside, we note that these bathymetric features do not appear to influence the location of the fronts in Drake Passage, as evident from the large temporal variability of the front locations shown in Figure 4. The generation mechanism of the eddies appears to be primarily through baroclinic instability near the fronts (Peterson *et al.,* 1982; Bryden, 1983), as suggested by the sea surface height extrema (Fig. 6). Although other eddy generation mechanisms, such as barotropic instabilities and mean current-bottom topography interaction, cannot as yet be discounted.

Spatial scale of the eddies from both the altimetric data and the XBT temperature sections range from 50–100 km in diameter, again supporting the need for closely spaced hydrography for resolution of upper ocean variability within Drake Passage. The altimetric data suggest time scales of ~35 days. Future studies will further explore the formation of the eddies, and quantify and characterize their impact on properties and transport through Drake Passage, by combining the complementary altimetric, XBT and XCTD data.

c. Drake Passage transport variability is highly correlated to southeast Pacific winds

To determine transport estimates from the XBT temperature measurements we derive a multivariate regression relationship between upper ocean temperature and a baroclinic mass transport function with an error of only 5–10 m^2. The difference in the mass transport function across the Drake Passage is of order 90 m^2. The five-year time series of total transport through Drake Passage shows substantial variability on interannual time scales, and commensurate with the positions of the fronts, no real seasonal signal is discernible. The temporal mean total transport value of 71 $\pm$ 15 Sv is of the same order as that determined from the earlier ISOS measurements in Drake Passage, relative to 2500 db.

While in the temporal mean, the strongest eastward transport is associated with the three major ACC fronts—the SAF, the PF and the SACCF—in Drake Passage, the individual cruises strongly suggest a banded nature to the flow through the passage. Some, although

not all, of the reversing bands of flow can be attributed to the presence of mesoscale eddy-type features within the APFZ. Alternating eastward and westward counterflows are evident in nearly all transects even when the temperature structure from Plate 1 does not directly indicate the presence of eddies. Upstream of Drake Passage at 88W, Donohue *et al.* (2001) noted the presence of five narrow jets across the ACC, separated by counterflow from an eddy north of the SAF, but also by other regions of weaker westward flow. Many of the current cores are only 50–100 km wide. The upper layer velocity cores were well resolved by Donohue *et al.*'s (2001) underway shipboard ADCP velocity measurements. In Drake Passage, the three major jets in the ACC were identified using the ISOS hydrographic CTD data (Nowlin *et al.,* 1977; Orsi *et al.,* 1995) which were typically separated by 50 km (for example, see Fig. 8). It may be that the 6–15 km spatial resolution of the XBT data is more readily capable of distinguishing the counterflows across Drake Passage than afforded by the typical 50 km resolution of the historical hydrographic sections.

The ISOS studies in Drake Passage revealed that variability in the ACC transport through Drake Passage is related to the wind field (Wearn and Baker, 1980; Peterson, 1988). Using the seven-day fields of scatterometer wind from the ERS 1 and 2 satellites, the zonally-averaged zonal wind stress between 55–60S (the latitude of Drake Passage) is not significantly correlated to the transport time series ($r = -0.28$), although the zonally averaged wind stress curl for the same latitude band is significantly correlated ($r = -0.63$) at the 99% level of significance (0.45). Spatially, the highest correlation with the Drake Passage XBT transport time series is for zonal wind stress (positive correlation) and wind stress curl (negative correlation) in the southeast Pacific Ocean (Fig. 12). This region is located just south of the zero wind stress curl contour, but north of the Orsi *et al.* (1985) defined SAF (Fig. 12). A positive wind stress curl in this region can contribute to the Sverdrup circulation within the subtropical gyre, and may therefore decrease transport towards Drake Passage. More likely the variations in the zonal wind stress in the southeast Pacific impart direct force on the ACC, and hence their high correlation with the ACC transport fluctuations. This is consistent with the positive sign of the correlation, implying that strong eastward winds are associated with strong eastward transport. Given that there are only 33 points in our time series, however, the significance of these correlations should be treated with caution.

d. Limitations of the study

The empirical relationship of the baroclinic mass transport derived here to show upper ocean variability in Drake Passage represents a first attempt. One of the main shortcomings of the technique is the inability to resolve transport in shallow water over the shelf. Whitworth and Peterson (1985) estimated a transport of 2 Sv over the north and south shelf regions (shallower than 2500 db) from moorings and pressure gauges during the ISOS period. The future inclusion of simultaneous salinity data from XCTD sampling on each XBT cruise in Drake Passage, can be used to directly determine the steric height and thus

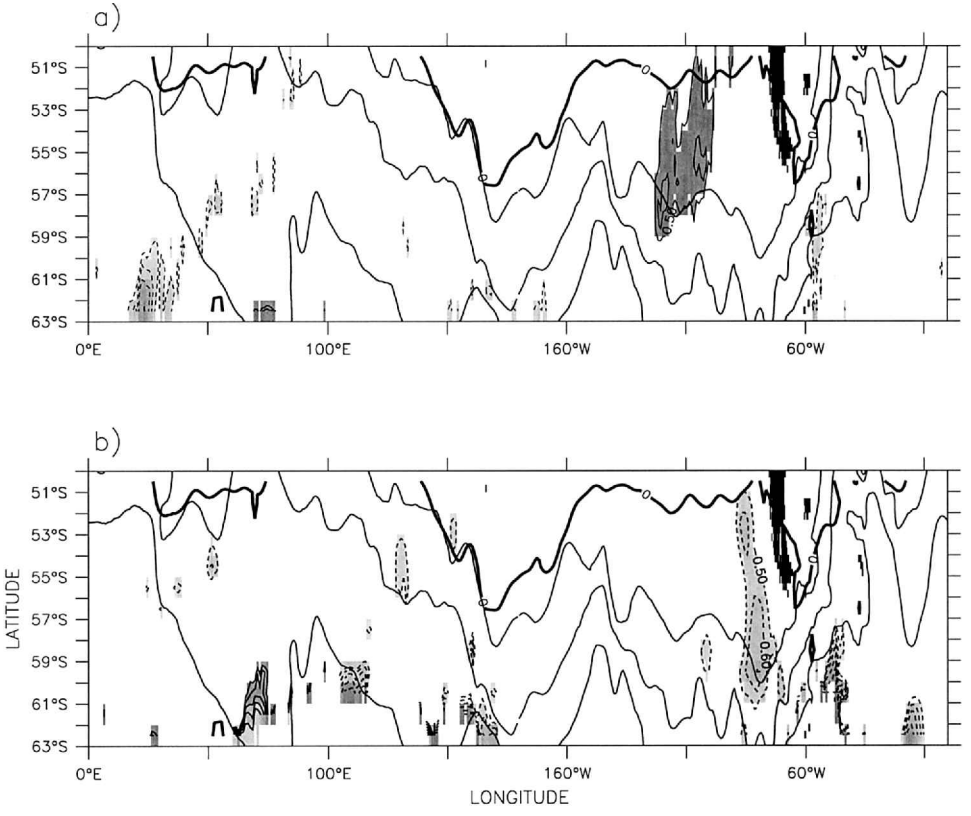

Figure 12. Contours of significant correlation (shaded) of the Drake Passage transport time series from the XBT data and the ERS scatterometer wind fields of (a) zonal wind stress and (b) wind stress curl. Correlations above 0.45 are significant at the 99% confidence limit. Also shown, are the contour of zero wind stress curl (line-0), and from north to south, the the location of the Subantarctic Front, Polar Front and the Southern Antarctic Circumpolar Current Front from Orsi *et al.* (1995).

reduce this error. In addition, the principal error in the true estimate of the steric height due to salinity variability at the time of each survey will also be directly accounted for.

Of course, the main problem with the XBT and XCTD probes in their use for baroclinic transport estimates in the Southern Ocean is the 800 m depth rating of the probes. Substantial geostrophic shear may exist at depth within the ACC that is not captured by the XBT/XCTD measurements if used solely to estimate the baroclinic flow. As a first cut, we have attempted to somewhat alleviate this deficiency and the lack of concurrent salinity data, by utilizing the high correlation between temperature at discrete depths and the 0–2500 db baroclinic transport function from the historical data. In future studies, it is expected that the altimetric sea surface height data will also provide a highly complementary measurement for examining transport variability through Drake Passage. The altimet-

ric sea surface height estimate includes the steric height that can be estimated from the XBT/XCTD data to 800 db, plus the baroclinic flow below the 800 db level of no motion assumed by that estimate, and the total barotropic effects. The barotropic contribution to the ACC has been determined primarily from bottom pressure measurements within Drake Passage during ISOS (Whitworth and Peterson, 1985). From their results, Whitworth and Peterson (1985) argued that variability in ACC transport is closely related to barotropic variability. More recently, Woodworth *et al.* (1996) found a significant correlation between the TOPEX/Poseidon altimetric measurements and bottom pressure sensors from the northern side of Drake Passage, although model results found this unrelated to transport variability through the passage. More importantly for transport variation however, significant rms differences between sea level and bottom pressure measurements were found in the south due to large baroclinic variability. Cunningham *et al.* (2003) showed that total transport across the six WOCE SR1 sections just east of Drake Passage could also be partitioned equally between baroclinic and barotropic components. They conclude, as do Woodworth *et al.* (1996), that supplementary *in situ* measurements are required in order for the altimeter to provide information directly relatable to total transport variability through Drake Passage. We suggest that the multi-year, bi-monthly sampling from the XBT and XCTD transects, combined with the 10-day repeat cycle from altimeter measurements, provides a powerful advantage for determining the upper ocean heat content, velocity and transport over a wide range of time and space scales within Drake Passage. This will be the subject of a future manuscript.

Acknowledgments. I would like to dedicate this paper to Ray Peterson, who helped initiate the high resolution XBT/XCTD program in Drake Passage. Ray was truly a pioneer in Southern Ocean studies and enthusiastically shared his vast experience and knowledge. His expansive legacy of significant papers are a testament to his collection and careful interpretation of Southern Ocean data. Because of the intense XBT sampling schedule and berthing limitations of the R/V *Gould,* this program relies on the assistance of the NSF-supported Raytheon Polar Services personnel (formerly the Antarctic Support Associates), and sometimes the cruise participants, to undertake the actual XBT sampling. Such assistance is genuinely appreciated and crucial to the continued success of the program. This work was supported by the National Science Foundation award OPP00-03618.

REFERENCES

Benada, J. R. 1997. Physical Oceanography Distributed Active Archive Center PO.DAAC Merged GDR (TOPEX/Poseidon). Users Handbook, Version 2.

Botnikov, V. N. 1963. Geographical position of the Antarctic Convergence Zone in the Southern Ocean. Information of the Soviet Antarctic Expedition (Eng. Trans), *4,* 324–327.

Bretherton, F., R. Davis and C. Fandry. 1976. A technique for objective analysis and design of oceanographic experiments applied to MODE-73. Deep Sea Res., *23,* 559–585.

Bryden, H. L. 1979. Poleward heat flux and conversion of available potential energy in Drake Passage. J. Mar. Res., *37,* 1–22.

Bryden, H. L. 1983. The Southern Ocean, *in* Eddies in Marine Science, A. R. Robinson, ed., Springer-Verlag, NY, 265–277.

Cunningham, S. A., S. G. Alderson, B. A. King and M. A. Brandon. 2003. Transport and variability of the Antarctic Circumpolar Current in Drake Passage. J. Geophys. Res., (in press).

Donohue, K. A., E. Firing and S. Chen. 2001. Absolute geostrophic velocity within the Subantarctic Front in the Pacific Ocean. J. Geophys. Res., *106,* 19869–19882.

Feng, M. and S. Wijffels. 2002. Intraseasonal variability in the South Equatorial Current of the East Indian Ocean. J. Phys. Oceanogr., *32,* 265–277.

Gaspar, P., F. Ogor, P.-Y. Le Traon and O. Z. Zanifé. 1994. Estimating the sea state bias of the TOPEX and Poseidon altimeters from cross-over differences. J. Geophys. Res., *99,* 24981–24994.

Gilson, J., D. Roemmich, B. Cornuelle and L. L. Fu. 1998. Relationship of TOPEX/Poseidon altimetric height to steric height and circulation in the North Pacific. J. Geophys. Res., *103,* 27947–27965.

Goni, G. J. and W. E. Johns. 2001. A census of North Brazil Current rings observed from TOPEX/Poseidon altimetry: 1992–1998. Geophys. Res. Lttrs., *28,* 1–4.

Gordon, A. L., D. T. Georgi and H. W. Taylor. 1977. Antarctic Polar Front zone in the western Scotia Sea—Summer 1975. J. Geophys. Res., *7,* 309–328.

Gordon, A. L. and H. W. Taylor. 1975. Heat and salt balance within the cold waters of the world ocean, *in* Numerical Models of Ocean Circulation, Natl. Acad. Sci., 54–56.

Hanawa, K., P. Rual, R. Bailey, A. Sy and M. Szabados. 1995. A new depth-time equation for Sippican or TSK T-7, T-6 and T-4 expendable bathythermographs (XBT). Deep-Sea Res. (1) *42,* 1423–1451.

Hofmann, E. E. and T. Whitworth. 1985. A synoptic description of flow at Drake Passage from year-long measurements. J. Geophys. Res., *90,* 7177–7187.

Joyce, T. M. and S. L. Paterson. 1977. Cyclonic ring formation at the Polar Front in the Drake Passage. Nature, *265,* 131–133.

Joyce, T. M., S. L. Paterson and R. C. Millard. 1981. Anatomy of a cyclonic ring in the Drake Passage. Deep-Sea Res., *28A,* 1265–1287.

Joyce, T. M., W. Zenk and J. M. Toole. 1978. The anatomy of the Antarctic Polar Front in Drake Passage. J. Geophys. Res., *83,* 6093–6114.

Legeckis, R. 1977. Oceanic Polar Front in the Drake Passage—Satellite observations during 1976. Deep-Sea Res., *24,* 701–704.

McCarthy, M., L. D. Talley and D. Roemmich. 2000. Seasonal to interannual variability from XBT and TOPEX/Poseidon data in the South Pacific subtropical gyre. J. Geophys. Res., *105,* 19535–19550.

McCartney, M. 1977. Subantarctic Mode Water, *in* A Voyage of Discovery, M. V. Angel, ed., Pergamon, NY, 103–119.

McDonald, A. 1998. The global ocean circulation: A hydrographic estimate and regional analysis. Prog. Oceanogr., *41,* 281–382.

Moore, J. K., M. R. Abbott and J. G. Richman. 1997. Variability in the location of the Antarctic Polar Front (90–20W) from satellite sea surface temperature data. J. Geophys. Res., *102,* 27825–27833.

Morrow, R. A., R. Coleman, J. A. Church and D. B. Chelton. 1994. Surface eddy momentum flux and velocity variance in the Southern Ocean momentum balance. J. Phys. Oceanogr., *24,* 2050–2071.

Nowlin, W. D., Jr. and M. Clifford. 1982. The kinematic and thermohaline zonation of the Antarctic Circumpolar Current at Drake Passage. J. Mar. Res., *40,* 481–507.

Nowlin, W. D., Jr., T. Whitworth and R. D. Pillsbury. 1977. Structure and transport of the Antarctic Circumpolar Current at Drake Passage from short-term measurements. J. Phys. Oceanogr., *7,* 788–802.

Nowlin, W. D., Jr. and W. Zenk. 1988. Westward currents along the margin of the South Shetland Island Arc. Deep Sea Res., *35,* 269–301.

Olbers, D., V. Gouretski, G. Seiss and J. Schroter. 1992. Hydrographic Atlas of the Southern Ocean, Alfred Wegener Institute, Bremerhaven, Germany.

Orsi, A. H., T. Whitworth and W. D. Nowlin. 1995. On the meridional extent and fronts of the Antarctic Circumpolar Current. Deep Sea Res., Part 1, *42,* 641–673.

Peterson, R. G. 1988. On the transport of the Antarctic Circumpolar Current through Drake Passage and its relation to wind. J. Geophys. Res., *93,* 13993–14004.

Peterson, R. G., W. D. Nowlin, Jr. and T. Whitworth III. 1982. Generation and evolution of a cyclonic ring at Drake Passage in early 1979. J. Phys. Oceanogr., *12,* 712–719.

Phillips, H. E. and S. R. Rintoul. 2000. Eddy variability and energetics from direct current measurements in the Antarctic Circumpolar Current south of Australia. J. Phys. Oceanogr., *30,* 3050–3076.

Pillsbury, R. D., T. Whitworth III, W. D. Nowlin, Jr. and F. Sciremammano, Jr. 1979. Currents and temperatures as observed in Drake Passage during 1975. J. Phys. Oceanogr., *9,* 469–482.

Ridgway, K. and J. S. Godfrey. 1994. Mass and heat budgets in the East Australian Current—a direct approach. J. Geophys. Res., *99,* 3231–3248.

Rintoul, S. R. 1991. South Atlantic interbasin exchange. J. Geophys. Res., *96,* 2675–2692.

Rintoul, S. R., J. R. Donguy and D. H. Roemmich. 1997. Seasonal evolution of upper ocean thermal structure between Tasmania and Antarctica. Deep-Sea Res., *44,* 1185–1202.

Roemmich, D. and B. Cornuelle. 1987. Digitization and calibration of the expendable bathythermograph. Deep-Sea Res., *34,* 299–307.

Roether, W., R. Schlitzer, A. Putzka, P. Beining, K. Bulsiewicz, G. Rohardt and F. Delahoyde. 1993. A chlorofluoromethane and hydrographic section across Drake Passage: Deep water ventilation and meridional property transport. J. Geophys. Res., *98,* 14423–14435.

Sciremammano, F., R. D. Pillsbury, W. D. Nowlin and T. Whitworth. 1980. Spatial scales of temperature and flow in Drake Passage. J. Geophys. Res., *85,* 4015–4028.

Sievers, H. A. and W. J. Emery. 1978. Variability of the Antarctic Polar Frontal zone in Drake Passage—Summer 1976–1977. J. Geophys. Res., *83,* 3010–3022.

Sievers, H. A. and W. D. Nowlin, Jr. 1988. Upper ocean characteristics in Drake Passage and adjoining areas of the Southern Ocean, 39W–95W, *in* Antarctic and Resources Variability, D. Sahrahag, ed., Springer-Verlag, Berlin, 57–80.

Smith, W. F. and D. T. Sandwell. 1997. Global sea floor topography from satellite altimetry and ship depth soundings. Science, *277,* 1956–1962.

Sprintall, J., D. Roemmich, B. Stanton and R. Bailey. 1995. Regional climate variability and ocean heat transport in the south-west Pacific Ocean. J. Geophys. Res., *100,* 15865–15871.

Wearn, R. B. and D. J. Baker, Jr. 1980. Bottom pressure measurements across the Antarctic Circumpolar Current and their relation to the wind. Deep-Sea Res., *27A,* 875–888.

Whitworth, T., III. 1980. Zonation and geostrophic flow of the Antarctic Circumpolar Current at Drake Passage. Deep-Sea Res., *27,* 497–507.

——1983. Monitoring the net transport of the Antarctic Circumpolar Current at Drake Passage. J. Phys. Oceanogr., *13,* 2045–2057.

Whitworth, T., III and W. D. Nowlin, Jr. 1987. Water masses and currents of the Southern Ocean at the Greenwich meridian. J. Geophys. Res., *92,* 6462–6476.

Whitworth, T., III, W. D. Nowlin, Jr. and S. J. Worley. 1982. The net transport of the Antarctic Circumpolar Current through Drake Passage. J. Phys. Oceanogr., *12,* 960–971.

Whitworth, T., III and R. G. Peterson. 1985. Volume transport of the Antarctic Circumpolar Current from bottom pressure measurements. J. Phys. Oceanogr., *15,* 810–816.

Woodworth, P. L., J. M. Vassie, C. W. Hughes and M. P. Meredith. 1996. A test of the ability of TOPEX/Poseidon to monitor flows through Drake Passage. J. Geophys. Res., *101,* 11935–11947.

Received: *14 May, 2002;* revised: *14 January, 2003.*